IOPscience iopscience.iop.org

Home Search Collections Journals About Contact us My IOPscience

Dynamics of *k*-core percolation

This article has been downloaded from IOPscience. Please scroll down to see the full text article.

2007 J. Phys. A: Math. Theor. 40 F581

(http://iopscience.iop.org/1751-8121/40/27/F02)

View the table of contents for this issue, or go to the journal homepage for more

Download details:
IP Address: 171.66.16.109
The article was downloaded on 03/06/2010 at 05:18

Please note that terms and conditions apply.

IOP FTC
IOP PUBLISHING JOURNAL OF PHYSICS A: MATHEMATICAL AND THEORETICAL

J. Phys. A: Math. Theor. **40** (2007) F581–F587 doi:10.1088/1751-8113/40/27/F02

FAST TRACK COMMUNICATION

Dynamics of *k*-core percolation

C L Farrow, P Shukla and P M Duxbury

Physics and Astronomy Department, Michigan State University, East Lansing, MI 48824, USA

E-mail: duxbury@pa.msu.edu

Received 18 April 2007
Published 20 June 2007
Online at stacks.iop.org/JPhysA/40/F581

Abstract

In many network applications nodes are stable provided they have at least k neighbours, and a network of k-stable nodes is called a k-core. The vulnerability to random attack is characterized by the size of culling avalanches which occur after a randomly chosen k-core node is removed. Simulations of lattices in two, three and four dimensions, as well as small-world networks, indicate that power-law avalanches occur in first-order k-core systems, while truncated avalanches are characteristic of second-order cases.

PACS numbers: 64.60.Ak, 05.70.Jk, 61.43.Bn, 46.30.Cn

(Some figures in this article are in colour only in the electronic version)

The k-core of a network is the set of nodes and edges which remain after all nodes which have less than k neighbours, and the edges attached to them, have been culled or removed. Percolation of k-cores has applications ranging from magnetism (where it was invented and called bootstrap percolation) [1, 2] and rigidity percolation [3, 4] to social networks [5] and protein networks [6], as well as the jamming transition [7]. The behaviour on Bethe lattices is particulary interesting due to the mixed nature of the transition where a first-order jump in the order parameter is co-existent with a square-root singularity [1, 3]. This behaviour has recently been associated with the jamming transition in granular media [7] and has been analysed using a $1/d$ expansion, which confirmed that it persists in finite dimensions [8], and by large scale simulations, which suggest that in four dimensions the transition is not mixed [9]. In general, k-core percolation in finite dimensions is quite different than that occuring on random graphs, with metastability being a key new feature, so that for $k > z/2$ hypercubic lattices have thresholds approaching one in the large lattice limit [10–14], whereas on Bethe lattices the k-core threshold occurs at values less than 1 for all $k \leqslant z - 1$ [1]. Moreover, on random graphs k-core percolation is first order for all $k > 2$ [1] whereas on triangular lattices and cubic lattices the transition is second order and in the connectivity percolation university class for $k = 3$ [15–20].

The vulnerability of networks to random node removal or attack has a variety of physical applications including radiation damage, species extinctions in biological networks and random outages or cascading failures in communication or transportation networks [21].

 © 2007 IOP Publishing Ltd Printed in the UK

There are also relations to avalanches in materials problems, including fracture and earthquakes [22, 23], and Barkhausen noise in magnetic materials [22, 24, 25]. In fact, bootstrap percolation is related to the weak disorder limit of one of the key models of disordered magnets, the random field Ising model (RFIM) [26].

In an earlier paper [27], we defined elementary culling avalanches (ECA) in k-core or bootstrap problems to be avalanches induced by random removal of one node on a stable k-core, which is a dynamical procedure analogous to that used in crackling noise simulations in random-field systems [22]. We showed that on triangular and cubic lattices the ECA distribution provides a sensitive indicator of the nature of the bootstrap transition, even in the slowly convergent second-order case $k = 3$ [15–20] and the metastable $k = 4$ case [10–14].

Here, we show that in systems ranging from small-world networks to regular lattices, including hypercubic lattices in four dimensions, the dynamics of k-core percolation falls into two classes: (i) second-order systems which have truncated avalanche distributions where the largest avalanche grows very weakly with system size and (ii) first-order systems where avalanches are power-law distributed and the largest avalanche is of the order of the system size, producing a first-order jump in the infinite cluster probability at percolation. In the case of Bethe lattices, power-law avalanches in first-order cases can be demonstrated explicitly [28] (see below).

Culling cascades for a variety of lattices in finite dimensions are presented in figures 1 and 2(a). These distributions are found by starting with a lattice with all sites present and then repeating two steps: (i) randomly remove a site and all edges connected to it, (ii) recursively cull all unstable sites until a stable k-core is achieved. The number of sites removed during step (ii) constitutes an elementary culling avalanche (ECA). The distribution of such avalanches, beginning with an undiluted lattice and continuing until the lattice is empty, yields the cummulative culling avalanche distribution, $C(a)$. We also monitor the largest avalanche that occurs for a given lattice, $a_{\max}$, which is the maximum cascade over the whole avalanche trace. The finite-size scaling behaviour of the maximum cascade is presented in the insets to figures 1 and 2(a).

In figure 1, we present avalanche distributions for $k = 3, 4, 5$, on eight-coordinated lattices in three (figure 1(a)) and four dimensions (figure 1(b)). These lattices where chosen to demonstrate the effect of spatial dimension on the nature of the k-core transition. It is clear from these data that the $k = 4$ transition changes from second order to first order as we go from three to four dimensions as noted recently [9]; however, the $k = 3$ transition is second order in both three and four dimensions. In contrast, on $z = 8$ Bethe lattices and random graphs, k-core percolation is first order for all $k > 2$. Clearly, dimension plays an important role on the nature of the k-core transition, moreover whenever the transition is first order we see the same characteristic behaviour: power-law avalanches and a largest avalanche of the order of the sample size [27].

We investigated a second method for changing the nature of k-core transitions, namely by changing the range of the interactions. To do this, we created small-world networks by starting with an undiluted triangular lattice and randomly removing a fraction f of bonds from it. These bonds are then randomly put back into the lattice, but they may connect any pair of sites at arbitrary distances, with the constraint that all sites remain six coordinated. In this way, we create six-coordinated small-world networks with fraction f of long-range connections. When f is zero, we have a regular triangular lattice, while when $f = 1$, we generate a random regular graph with coordination six everywhere. By varying f, we monitor the effect of long-range connections on the nature of the k-core transition, which also measures the vulnerability of the small-world networks to random attack [21]. For $k = 3$, we find that, as illustrated in figure 2(a), the transition changes from second order to first order when the

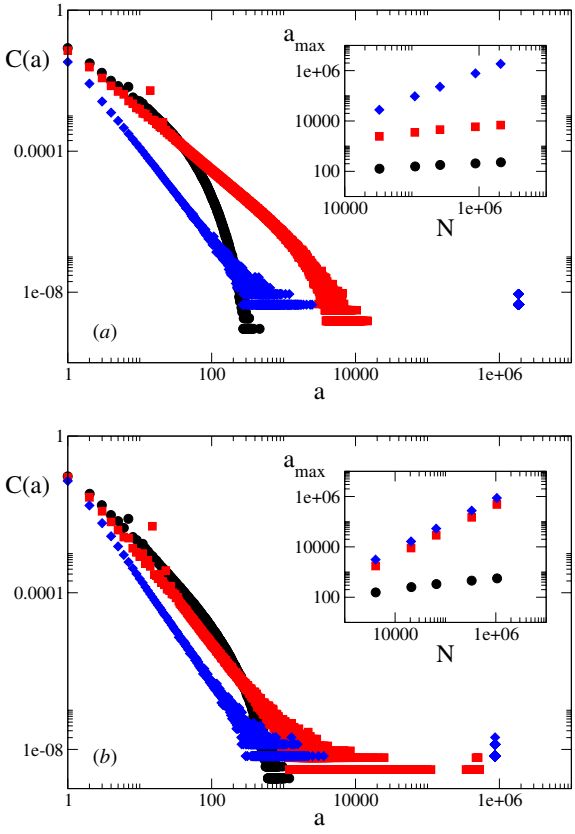

Figure 1. Effect of lattice dimension (d), at fixed lattice coordination (8), on the avalanche distribution (ECA), $C(a)$, for the cases $k = 3$ (black circles), $k = 4$ (red squares) and $k = 5$ (blue diamonds). (a) Body-centred cubic lattices ($d = 3$) and (b) simple cubic lattices ($d = 4$). The 4-core transition changes from second order for $d = 3$ to first order for $d = 4$ [9], as is clearly seen in the avalanche distributions and in the finite-size scaling of the largest avalanche, $a_{\max}$ (Insets). In (a) 1000 samples were used, and in the main figure the lattice size $L = 128$. In (b) 1000 samples were used, and in the main figure $L = 32$.

fraction of small-world connections reaches $f_c = 0.23(2)$. For $f > f_c$, there are power-law avalanches and an extensive largest avalanche, while for $f < f_c$, the avalanche distribution is truncated, with no large avalanches.

The 4-core transition on six-coordinated networks is first order for all f, however on triangular lattices it is metastable so that for large lattices the threshold approaches one very slowly, while on random graphs there is a finite threshold $p_c < 1$. Nevertheless, we find power-law avalanches and an extensive largest avalanche in all of these cases. However, the behaviour of the k-core threshold as a function of the fraction of small-world connections is interesting and is presented in figure 2(b). A notable feature of these data is that small-world connections quickly stabilize the metastable 4-core of triangular lattices and, as is emphasized in the inset to figure 2(b), there is a singular behaviour in $p_c(f)$ as $f \to 0$. Presumably, this non-perturbative behaviour is related to the stabilization of large holes in the triangular lattice by the addition of long-range loops characteristic of small-world networks, and it may be possible to characterize this behaviour using rigorous mathematical methods [10–13].

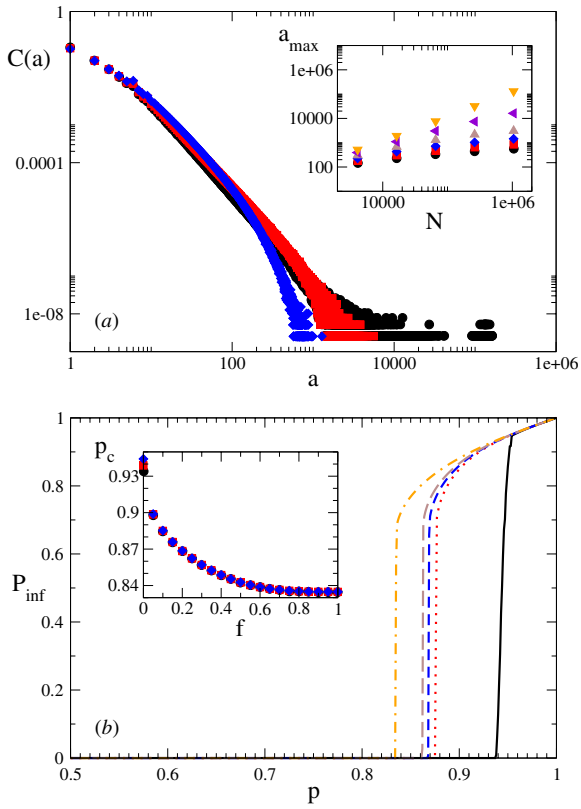

Figure 2. k-core percolation on six coordinated small-world networks, with fraction f of small-world connections. (a) Avalanche distributions, $C(a)$, for 3-core cases with $f = 0.15$ (blue diamonds), $f = 0.20$ (red squares) and $f = 0.25$ (black circles). Inset: the largest avalanche, $a_{\max}$, starting at the bottom, for $f = 0.15, 0.17, \ldots, 0.25$. ($b$) The infinite 4-core probability, $P_{\inf}$, versus site probability p for small-world fractions (from right to left) $f = 0, 0.15, 0.20, 0.25, 1$. Inset: the bootstrap percolation threshold, $p_c(f)$. There is a singular behaviour in $p_c(f)$ as $f \to 0$ (see the text). In the main figures of (a) and (b) and in the inset to (a) 1000 samples were used for each f, with $L = 1028$. In the inset to (b) 100 samples were used for $L = 256$ (black circles), $L = 512$ (red squares) and $L = 1024$ (blue diamonds).

We also observed power-law avalanches and an extensive largest avalanche in the limit $f = 1$ which is the random graph limit. In this limit, power-law avalanches can be demonstrated explicitly using Bethe lattices, as we now show. Consider site-diluted, z-coordinated Bethe lattices where a fraction p of the nodes are randomly removed, and let T be the branch probability that a node of the Bethe lattice is part of a k-core. The branch probability, T, is found by solving the self-consistent equation

$$T = p \sum_{n=k}^{z-1} A_n^{z-1} T^n \qquad \text{with} \qquad A_l^r = \binom{r}{l} (1-T)^{r-l}, \tag{1}$$

which is well known from the original bootstrap paper [1] and from applications to rigidity percolation [3]. The branch probabilities are used to find the probability of a site being on the k-core,

$$X = p \sum_{n=k}^{z} A_n^z T^n. \tag{2}$$

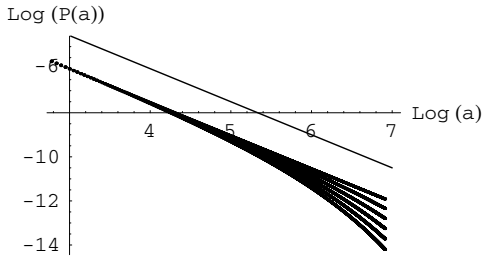

Figure 3. A log–log plot of culling avalanches, $P(a)$ for 3-core percolation on a $z = 4$ Bethe lattice, found from $P^*(y)$ (see the text after equation (8) using an exact Mathematica algorithm). The dark lines are for five values of the site concentration, from the top starting with $p = 8/9 = p_c$ and then moving above p_c in increments of $\delta p = 10^{-4}$. The continuous line of slope 3/2, vertically shifted from the data, is included to demonstrate that $P(a) \sim 1/a^{3/2}$ at the 3-core threshold, p_c.

We build on the results (1) and (2) to find the culling avalanche distributions for a branch, $B(a)$, and for the Bethe lattice, $P(a)$. $P(a)$ is the differential probability and is related to the cummulative probability, $C(a)$, through $C(a) = \int P(a, p)\,\mathrm{d}p$.

As noted previously [28, 29], sites which have exactly k neighbours play a special role in culling avalanches on Bethe lattices. Following their terminology, we define the corona as a connected cluster of sites each of which is part of the k-core and has exactly k neighbours. With this definition, removal of a site of the k-core leads to a culling avalanche in the corona surrounding that site. The probability of finding a corona of size, a, surrounding a randomly chosen starting site on the Bethe lattice is given by

$$P(a) = p \sum_{n=k}^{z} A_n^z \prod_{l=1}^{n} \sum_{a_l} B(a_l)\delta(S_n), \tag{3}$$

where $S_n = \sum_{l=1}^{n} a_l - a + 1$. This expression has the same form as equation (2), but with the term T^n in that equation replaced by the product in equation (3). This term is a product over the probabilities of finding corona on each of the branches connected to the starting site, and the delta function ensures that the ECA's on these corona sum to the total avalanche size a. From this equation it is evident that the normalizations $\sum P(a) = X$ and $\sum B(a) = T$ hold. A similar reasoning is applied to the branch probabilities, yielding the extension of equation (1) to

$$\frac{B(a)}{p} = \sum_{n=k}^{z-1} A_n^{z-1} T^n \delta(a) + A_{k-1}^{z-1} \prod_{l=1}^{k-1} \sum_{a_l} B(a_l)\delta(S_{k-1}). \tag{4}$$

There are two terms in this expression, as only corona sites on a branch initiate a culling avalanche on the branch. All other k-core sites terminate the ECA and contribute to the prefactor of $\delta(a)$ in this equation. This delta function is not present in equation (3) as the starting site there is removed by hand to initiate an ECA so it can have any coordination. Defining the generating functions, $B(y) = \sum B(a)y^a$ and $P(y) = \sum P(a)y^a$, and applying them to equation (3) yields

$$P(y) = py \sum_{n=k}^{z} A_n^z B(y)^n. \tag{5}$$

Similarly, equation (4) becomes

$$B(y) = p\sum_{n=k}^{z-1} A_n^{z-1} T^n + pyA_{k-1}^{z-1} B(y)^{k-1}. \tag{6}$$

The probabilities $B(a)$ or $P(a)$ are extracted from the generating functions $B(y)$ or $P(y)$, by differentiation or by contour integration, whichever is more convenient.

The cases $k = 1, 2$ are the standard connectivity percolation and percolative backbone problems, respectively, so the simplest non-trivial k-core problem on random graphs is $k = 3, z = 4$. The formalism outlined above can be carried out explicitly in this case and has a behaviour characteristic of all cases $k \geqslant 3$ [28, 29]. For this case, $B(y)$ obeys

$$B(y) = pT^3 + 3py(1-T)B(y)^2, \tag{7}$$

where $T = 3/4 + 9(\delta p)^{\frac{1}{2}}/8\sqrt{2}$, which follows from equation (1) and $\delta p = p - p_c$. This illustrates the characteristic feature of a jump discontinuity and a continuous square-root singularity, as noted before [1, 3]. Solving equation (7) and selecting the physical root, we find an explicit expression for the avalanche generating function,

$$B^*(y) = \frac{1 - [1 - 12p^2T^3(1-T)y]^{\frac{1}{2}}}{6p(1-T)y} \tag{8}$$

and finally, from equation (4), we find the generating function for Bethe lattices, $P^*(y) = py[4(1-T)B^*(y)^3 + B^*(y)^4]$. We wrote a Mathematica program which finds the exact culling avalanche distribution from $P^*(y)$, and the results are presented in figure 3, which demonstrates the 3/2 power-law behaviour at threshold characteristic of mean-field avalanches. Asymptotic analysis near criticality is carried out by noting that the normalization condition $B^*(y = 1) = T$ enables an expansion of B^* near $y = 1$ and $p = p_c$. The leading term in the expansion of B^* is then $B^* \approx 1 - [1 - y(1 + 9\delta p/2)]^{1/2}$, from which we find that near the threshold, p_c, the tail of the avalanche distribution obeys $P(a) \sim [1 - D(p - p_c)]^a/a^{3/2}$, where $D = 9/2$ and $p_c = 8/9$ for 3-core percolation on four-coordinated Bethe lattices. In experiments as well as computer simulations, it is more convenient to measure the integrated probability distribution of avalanches $C(a)$, and in the simulation results presented above we integrate over the complete avalanche trace. The probability of large avalanches is significant in a small region of width $\frac{1}{\delta p}$ near threshold. Integration of $P(a)$ in this regime yields $C(a) \sim a^{-\frac{5}{2}}$, for $a \to \infty$ which is observed in our simulations on random graphs, and is typical of avalanches occuring in infinite range models and Bethe lattices in a wide variety of non-equilibrium systems [22, 23, 29–31].

In all cases, we studied that power-law avalanches are associated with first-order k-core transitions, both in metastable and regular first-order cases. This is not without precedent as in random field Ising hysteresis a first-order jump occurs in the hysteresis loop despite the fact that power-law avalanches occur [22, 24]. However, in brittle fracture problems in finite dimensions, the avalanches are truncated when the load sharing is short ranged [32, 33]. Presumably, this is due to the greater amplification of stress on survivors in fracture problems with short-range load sharing. Nevertheless, k-core dynamics capture the essential physics of instabilities in a broad class of complex network problems.

References

[1] Chalupa J, Leath P L and Reich G R 1979 *J. Phys. C: Solid State Phys.* **12** L31
[2] Kogut P M and Leath P L 1981 *J. Phys. C: Solid State Phys.* **14** 3187
[3] Moukarzel C, Duxbury P M and Leath P L 1997 *Phys. Rev.* E **55** 5800

[4] Duxbury P M, Jacobs D J, Thorpe M F and Moukarzel C 1999 *Phys. Rev.* E **59** 2084
[5] Seidman S B 1983 *Soc. Netw.* **5** 269
[6] Wuchty S and Almaas E 2005 *Proteomics* **5** 444
[7] Schwarz J H, Liu A J and Chayes L Q 2006 *Europhys. Lett.* **73** 560
[8] Harris A B and Schwarz J M 2005 *Phys. Rev.* E **72** 46123
[9] Parisi G and Rizzo T 2006 *Preprint* Cond-mat 609777
[10] Aizenman M and Lebowitz J L 1988 *J. Phys. A: Math. Gen.* **21** 3801
[11] Shonmann R H 1992 *Ann. Probab.* **20** 174
[12] Cerf R and Manzo F 2002 *Stoch. Process Appl.* **100** 69
[13] Holroyd A E 2003 *Probab. Theory Relativ. Fields* **125** 195
[14] DeGregorio P, Lawlor A, Bradley P and Dawson K A 2004 *Phys. Rev. Lett.* **93** 25501
[15] Chaves C M and Koiller B 1995 *Physica* A **218** 271
[16] Medeiros M C and Chaves C M 1997 *Physica* A **234** 604
[17] Stauffer D and de Arcangelis L 1996 *Int. J. Mod. Phys.* C **7** 739
[18] Branco N S and Silva C J 1999 *Int. J. Mod. Phys.* C **10** 921
[19] Adler J and Lev U 2003 *Braz. J. Phys.* **33** 641
[20] Kurtsiefer D 2003 *Int. J. Mod. Phys.* C **14** 529
[21] Albert R, Jeong H and Barabasi A L 2000 *Nature* **406** 378
[22] Sethna J P, Kahmen K A and Myers C R 2001 *Nature* **410** 242
[23] Alava M J, Nukala P K V V and Zapperi S 2006 *Adv. Phys.* **55** 349
[24] Dahmen K A, Sethna J P, Kuntz M C and Perkovic O 2001 *J. Magn. Magn. Mater.* **226** 1287
[25] Durin G and Zapperi S 2000 *Phys. Rev. Lett.* **84** 4705
[26] Sabhapandit S, Dhar D and Shukla P 2002 *Phys. Rev. Lett.* **88** 197202
[27] Farrow C, Moukarzel C F and Duxbury P M 2005 *Phys. Rev.* E **72** 66109
[28] Dorogovtsev S N, Goltsev A V and Mendes J F F 2006 *Phys. Rev. Lett.* **96** 40601
[29] Goltsev A V, Dorogovtsev S N and Mendes J F F 2006 *Phys. Rev.* E **73** 56101
[30] Kloster M, Hansen A and Hemmer P C 1997 *Phys. Rev.* E **56** 2615
[31] Vespignani A and Zapperi S 1998 *Phys. Rev.* E **57** 6345
[32] Zapperi S, Nukala P K V V and Simunovic S 2005 *Phys. Rev.* E **71** 26106
[33] Hidalgo R C, Moreno Y, Kun F and Herrmann H J 2002 *Phys. Rev.* E **65** 46148